Permafrost Detection with Remote Sensing and Geophysics on the Tibetan Plateau

Eike Reinosch, Johannes Buckel, Markus Gerke, Andreas Hördt, Jussi Baade & Björn Riedel

In this study we combine geophysical techniques in the form of microwave remote sensing and Electrical Resistance Tomography (ERT) interferometry to study the extent of permafrost in the catchment of Lake Nam Co on the Tibetan plateau. Interferometric Synthetic Aperture Radar (InSAR) is a powerful technique to monitor permafrost related surface displacement processes on a large scale. However, the insensitivity of InSAR data regarding northward or southward directed motion and its inability to detect permafrost when no displacement occurs, impose significant limitations to its application in permafrost study. We highlight those limitations on a rock glacier within Qugaqie basin, a sub-catchment within the Nyainqêntanglha range, and show how ERT can be used to compensate for them. With this combined approach we will create an inventory of rock glaciers and constrain the extent of permafrost areas within the Nyainqêntanglha range.
keywords: Permafrost, Remote Sensing, Geophysics, Tibetan Plateau

1. Introduction

Studying permafrost landscapes and their related processes is of immense importance as they act as both carbon sinks and water storages (Hock et al. 2019). The degradation of permafrost is a severe problem, as this releases the stored carbon to the air to accelerate climate change and destabilizes the ground, leading to soil erosion and slope collapses in mountain regions (Haeberli et al. 2010). The air temperature on the Tibetan Plateau has been shown to rise significantly faster than the global average (Yao et al. 2000), which has contributed to permafrost degradation throughout the plateau (Wu et al. 2010). Interferometric Synthetic Aperture Radar techniques make it possible to study even remote permafrost landscapes and their related surface displacement processes on vast spatial scales. These observed motion patterns include seasonal signals induced by thawing of the ground in spring and subsequent refreezing in autumn, as well as multiannual creeping motions on the order of millimeters to decimeters per year. However, despite the obvious potency of InSAR to study these landscapes, this technique has some limitations. Heavy snowfall in winter can hide the surface from the satellite, making continuous monitoring impossible. In addition, InSAR data allows only to analyze motion towards the satellite or away from it and the multitude of atmospheric interference prevalent especially in high mountain areas creates noise. It is therefore crucial, to validate remote sensing data with field observations and measurements.

In this study we assess the potential of combining geophysical techniques, such as Electrical Resistance Tomography, with InSAR remote sensing analysis to detect long-term subsurface ice content and permafrost related landscapes on the Tibetan Plateau. To that end we highlight their interaction on a rock glacier within our study area, the Quagaqie basin at Lake Nam Co, and show how this approach can be used to detect other permafrost related landscapes on a larger scale.

2. Study Area

Our study area, the Qugaqie basin, covers 58 km² within the western Nyainqêntanglha range and features elevations of 4722 m to 6117 m a.s.l (Fig. 1A). This catchment was formed by glacial processes and as such is largely covered by unconsolidated glacial and periglacial deposits interspersed with grassland where soil has accumulated (Fig. 1B). Higher order vegetation is almost nonexistent and many slopes are not vegetated and prone to seasonal sliding (Reinosch et al. in review). The higher reaches of the catchment feature both active and inactive periglacial landforms, such as rock glaciers. Rock glaciers are steadily creeping permafrost landforms of ice-rich debris in mountainous valleys (Haeberli et al. 2006). The main river is fed by hanging valleys, some containing the remnants of small glaciers, as well as the two main glaciers Zhadang and Genpu to the south.

The sparse snow cover in winter and the lack of vegetation make this region a suitable study site for periglacial processes using InSAR technology, as this reduces the risk of temporal decorrelation. However, temporal decorrelation remains a large issue during the thawing and freezing periods, when surface characteristics change rapidly over a few weeks, especially in areas with significant soil and grassland. Sentinel-1 is a suitable satellite system to study this region, due to its large footprint, relatively short revisit time and C-Band (5.6 cm) wavelength, which is less prone to decorrelation than shorter wavelengths (Crosetto et al. 2016).

3. Data and Methods

Here we use Sentinel-1 Level-1 single look complex data for all InSAR analysis, both from ascending and descending orbits from the interferometric wide swath mode with a ground resolution of 20 m azimuth and 5 m in range direction (ESA 2012) and a 12 day repeat interval in this region. Due to the unreliability of early Sentinel-1a data, we decided to start our time series analysis of our study area in May and November 2015 for ascending and descending acquisitions respectively. The latest data acquisitions included in the analysis are from December 2018. We used a total of 74 acquisitions in ascending and 63 acquisitions in descending orbit for our 3 year time series analysis. We carefully analyzed all individual interferograms and excluded those with long temporal or geometric baselines, unwrapping errors and overall low coherence and therefore poor spatial coverage. This especially excluded many acquisitions from spring to autumn, as freezing and thawing of the ground changes surface characteristics and overall surface change, including surface

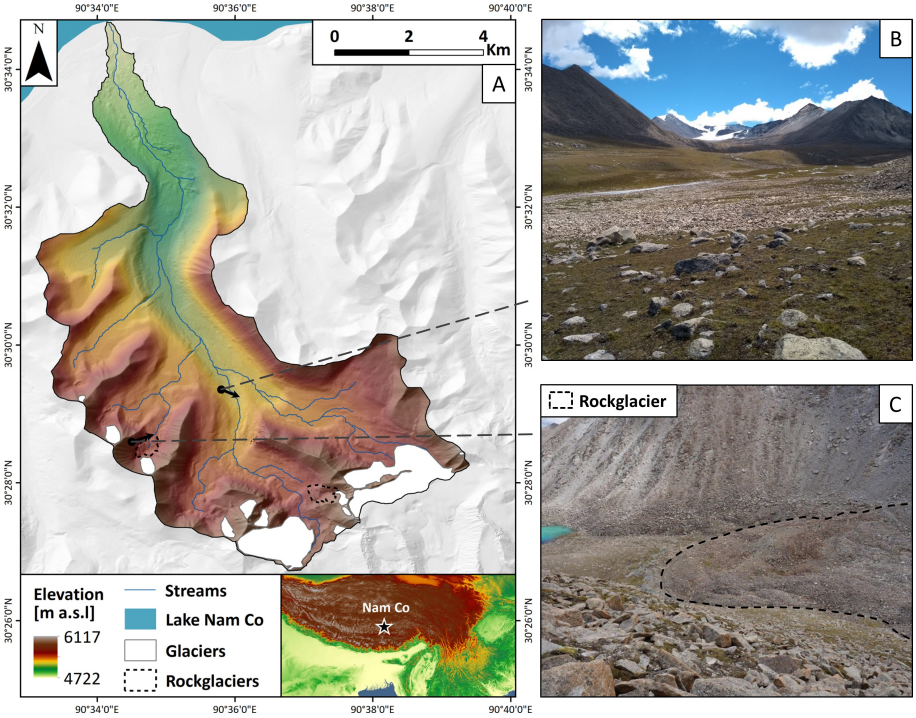

Figure 1: Overview map of the Qugaqie catchment at Lake Nam Co including the location of the study area on the Tibetan Plateau. Elevation data based on SRTM v4 (Jarvis et al. 2008) and TanDEM-X 0.4" DEM (©DLR 2017). The location and viewing direction of the images B and C are shown as black arrows. B: Image of the main valley of Qugaqie basin with the Zhadang glacier in the background. C: Image of the studied rock glacier (Fig. 2).

motion, is strongest during this time period. We chose a coherence threshold of 0.3 for our analysis.

Electrical resistivity tomography (ERT) is a widely used method in geoscience. It is especially potent for the detection of subsurface ice under permafrost conditions. It has been used to detect permafrost in loose sediments, including rock glaciers, since the end of the 1990s (Hauck and Von der Mühll 2003; Kneisel et al. 2008; Mewes et al. 2017; Von der Mühll et al. 2002). Geoelectric exploit the different electrical resistivities (or electrical conductivity as their reciprocal value) in the subsurface. The resistivity is generally higher in sediments interspaced by ice than in unfrozen bedrock and decreases significantly with increasing moisture content. The simplest iteration of this technique works with as little as four electrodes. Two electrodes feed current into the underground and generate an electric field in the subsurface, while two potential probes in between register the drop in voltage. These multi-channel geoelectric measurements result

in two-dimensional depth sections (so-called pseudo-sections), which show the distribution of the apparent resistances in the subsurface.

3.1. ERT data acquisition

The shown ERT results were acquired during the field trip in July 2018. We worked with multi-electrode equipment (50 electrodes), a maximum spacing of 2 meters and applied the roll-along procedure. Blocky surfaces like rock glaciers have difficult characteristics due to their instability and a lack of fine material required for the electricity feed to reach the ground. The best connection was accomplished in areas where sandy soil material filled the gaps between boulders. The ends of the electrodes were pushed through sponges into the fine material. We saturated the sponge with salted water, which kept the fine material wet due to desiccation through high solar radiation and supported a better electrode coupling and current-flow. We processed our ERT-data with the Res2Dinv-Software.

3.2. ISBAS Processing

We chose a modified version of the Small BAseline Subset (SBAS) method (Berardino et al. 2002) for our time series analysis, as tests showed that results from this approach are superior in terms of spatial coverage and noise level to Persistent Scatterer Interferometry (PSI). The SBAS method generates interferograms between SAR acquisitions with a short temporal and geometric baseline and stacks them to estimate surface displacement and velocity over a time period. Interferograms are a spatial representation of the phase difference of two SAR acquisitions and can be used to determine the relative surface displacement between them. The modified SBAS approach we employed, referred to as Intermittent SBAS (ISBAS) (Batson et al. 2015), produces a significantly improved spatial coverage by allowing limited interpolation of temporal gaps for areas, where the coherence is intermittently below the chosen threshold. Areas where at least 75% of interferograms feature a coherence above a threshold of 0.3 will be retainedin the final result. Those time periods when the coherence fell below the threshold were interpolated based on spatial and temporal parameters. This helped us to compensate for the lower coherence in spring to autumn, while still producing a reliable result. The topographic phase was removed from the interferograms with the TanDEM-X 12 m resolution DEM and the orbital phase was corrected via a polynomial function prior to unwrapping.

3.3. InSAR Postprocessing

The relative nature of InSAR results can make it difficult to interpret the results, especially in a dynamic mountainous setting. It is therefore desirable to derive absolute displacement signals by combining different data sets, such as ascending and descending orbits or field measurements, and by making a number of assumptions regarding the expected direction of the surface motion. The decomposition method combines ascending and descending acquisitions to derive absolute east-west and vertical displacement vectors but assumes

north-south displacements to be negligible (Fialko et al. 2001), due to the low sensitivity of SAR acquisitions in those directions. This popular technique is therefore not useful to us as it does not produce representative data for slopes with a north or south aspect. We instead employed a different method to estimate absolute surface velocity. Areas with a slope > 5 were projected in the direction of the steepest slope (after Notti et al. 2014), as most surface displacement is assumed to be caused by sliding processes transporting material parallel to the slope. This technique originates in landslide studies, where the direction of the landslide generally follows the steepest slope. We calculate a coefficient (C) in order to estimate the downslope velocity (V_{SLOPE}). C receives a value between 0.2 and 1, based on the cosine of the LOS (nlos, hlos and elos) of the satellite, calculated from the incidence angle (α) and the azimuth (θ) in radians, and the aspect (A) and slope (S) of the surface area. The LOS velocity (V_{LOS}) is the divided by C to produce the slope velocity. The following equations describe the necessary calculations to estimate the slope velocity (Notti et al., 2014):

$$V_{SLOPE} = V_{LOS}/C;$$
$$C = (nlos \cdot cos(S) \cdot sin(A - 1.571)) + (elos \cdot (-1 \cdot cos(S) \cdot cos(A - 1.571)) + (hlos \cdot sin(S)));$$
$$hlos = cos(\alpha); nlos = cos(1.571 - \alpha) \cdot cos(\eta); elos = cos(1.571 - \alpha) \cdot cos(\omega);$$
$$\eta = 3.142 - \Theta; \omega = 4.712 - \Theta.$$

The larger the difference between the LOS vector and the downslope vector, the smaller and therefore stronger C becomes. We excluded data points with a strong coefficient if a slope has a strong coefficient in only one LOS but not the other, as a strong coefficient is associated with a larger uncertainty. The maximum strength of C is set to 0.2 to avoid producing unrealistically large slope velocities caused by a coefficient close to zero. We used a smoothed version of the TanDEM-X DEM (with a 90 x 90 m moving mean) to determine the motion direction. We did this as we assume, that structures such as rock glaciers and landslides move a larger amount of sediment in a similar direction and we wanted to avoid outliers caused by single pixels with different slope aspects. This is a simplified approach to estimate the slope velocity and it does not take into account rotational and compressional motion within the moving structure. This approach is therefore likely to lead to an overestimation of the actual velocity in many areas.

4. Results and Discussion

We can clearly see from the results of our time series analysis, that the studied rock glacier is active. It shows clear creeping motion on the order of 5 to 15 cm/yr after our projection along the steepest slope (Fig. 2C). The outline of the rock glacier was derived from optical satellite data (©Bing 2019) and a 12 m resolution TanDEM-X DEM (©DLR 2017). We observe strong differences in velocity between different parts of the rock glacier but it is likely that this is not only a reflection of different levels of activity but rather due to varying surface aspects. When we compare the velocities to the surface

aspect, we can clearly see that those parts of the rock glacier with strong north or south aspects appear significantly less uniform and with more noise. This is connected to the low sensitivity of SAR acquisitions in the north-south direction due to the polar orbit of the satellite.

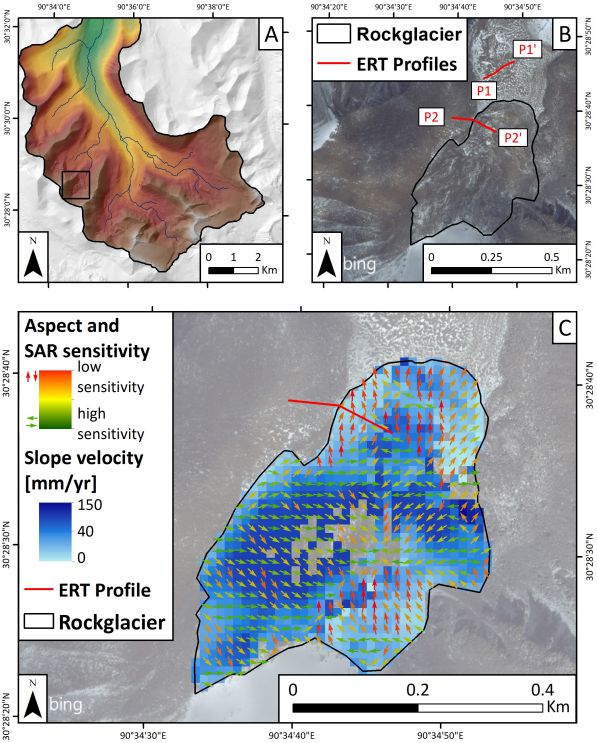

Figure 2: Overview of the study area (©DLR 2017) featuring the location of the rock glacier displayed in B and C. B: Extent of a rock glacier within the study area and the locations of our ERT profiles (Fig. 3) superimposed over an optical satellite image (©Bing 2019). C: Surface velocity of the rock glacier from 2015 to 2018 derived from ascending and descending Sentinel-1 satellite data (©Copernicus 2017). The velocity has been projected into the direction of the steepest slope (after Notti et al. 2014). The aspect of the surface is shown by arrows, colour coded according to the sensitivity of SAR acquisitions to those directions. The missing velocity values in the center of the rock glacier are likely caused by rotation of the surface material, which leads to decorrelation of the data.

The sensitivity coefficient we use to project our velocity models from LOS to the downslope direction, is strongest for slopes with a north or south aspect. Therefore the precision of our data is also lowest on those slopes, making the results more noisy in comparison to slopes with better sensitivity coefficients. Slopes with a strong coefficient also display overall lower slope velocities, like in the frontal region of the rock glacier, which again is

more indicative of the insensitivity of the satellite, rather than actually reduced velocities. This is corroborated by the ERT profile, which displays a cross-section of the frontal part of the rock glacier (Fig. 3, profile 2). Red and purple areas represent high resistivity (>100 kΩm), associated with subsurface ice content, while blue areas feature lower resistivity (<100 kΩm), associated with unfrozen ground. We positioned profile 1 (Fig. 3, profile 1) in front of the rock glacier in order to highlight the difference between frozen sediment of the rock glacier and partly frozen glacial till. In profile 1 we observe only individual ice lenses with similar high resistivity values (>70kΩm).

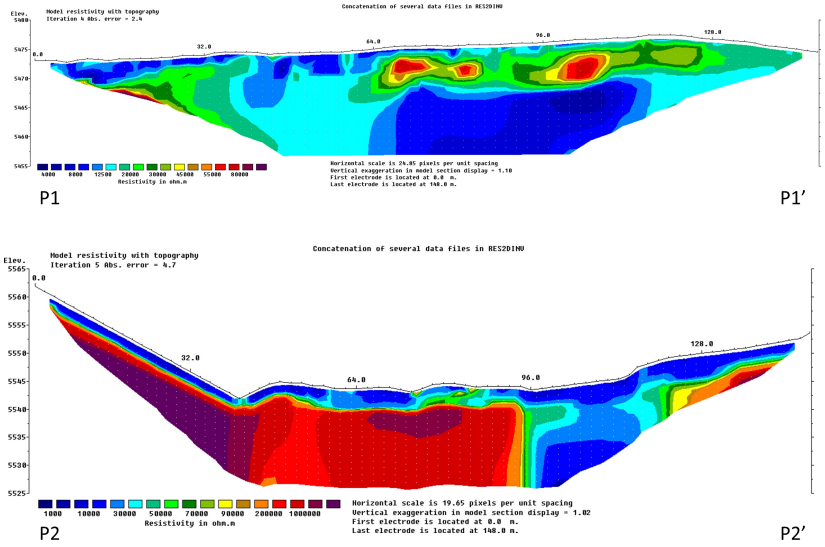

Figure 3: ERT profiles near the rock glacier shown in Fig. 2 B/C. Top: Profile 1 is characterized by low resistivity vales (<20 kΩm) associated with unfrozen ground dominated by conductive material. Three areas of higher resistivity values (>70 kΩm) are interpreted as ice lenses. Below: In profile 2 the uppermost, unfrozen layer represents the active layer (<20 kΩm), which thaws in summer. The black dashed line indicates frozen bedrock, while the high resistivity values (>70 kΩm) outside of the dashed line represent the frozen sediment of the rock glacier

Another limitation is that absence of permafrost related creep does not mean absence of subsurface ice. Areas with a small slope (<5°) rarely display surface creep (Daanen et al. 2012), yet they may still contain ice lenses and be categorized as permafrost. This is the case for the valley bottom in front of the rock glacier, where no significant creep takes place but where our ERT measurements nonetheless display ice content (Fig. 3, profile 1). Seasonal freezing and thawing cycles can also be observed in flat terrain but we could not observe a significant difference between cycles in areas with permafrost compared to areas with seasonally frozen ground, as both produce a similar freeze-thaw signal. It is therefore possible to use InSAR to detect permafrost where measureable creep takes place but using it to identify permafrost on flat ground or on north- or south-facing slopes is

problematic. Despite these limitations InSAR time series analysis is still a capable tool when it comes to studying permafrost creep, as it can be used to identify rock glaciers and other periglacial landforms with sufficiently large motion over extended areas. It should therefore be used in combination with optical satellite data and geomorphological maps to determine the extent of such landforms after they have been detected with InSAR. We aim to expand our approach to a larger region, in this case the northern Nyainqêntanglha range, to assess its viability on a regional scale (Fig. 4).

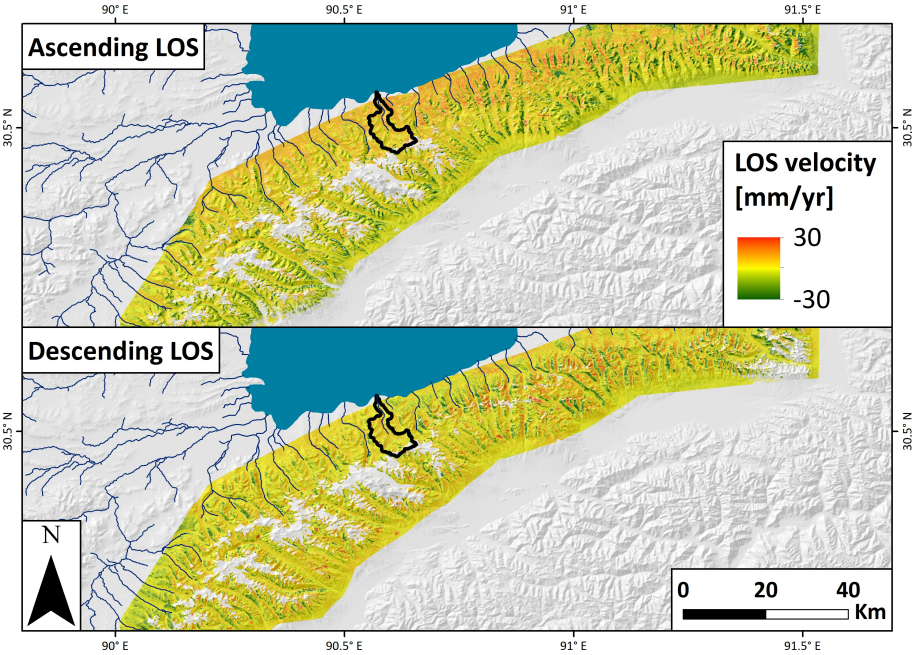

Figure 4: Preliminary results of InSAR time series analysis of the Nyainqêntaglha mountain range from 2015 to 2019 based on Sentinel-1 data (©Copernicus 2017). The outline of Qugaqie basin (Fig. 1) is shown in black.

5. Summary and Outlook

Our combination of geophysical field measurements and microwave remote sensing highlights the capabilities of each technique and how they can be used in combination to compensate for their limitations for permafrost investigation. InSAR time series analysis allows us to detect surface motion induced by permafrost creep on a large scale, while ERT measurements add information about permafrost areas without significant surface creep and slopes where InSAR sensitivity is low i.e. with a strong north or south aspect.

We studied a rock glacier within the Qugaqie basin extensively with both techniques, with the goal of applying this detailed information to the entire Nyaingêntaglha range to create an inventory of permafrost related creep processes and to better constrain the permafrost extent in this area. Further validation with TerraSAR-X satellite data and ground-truth through terrestrial laser scans will be added to our models to improve their precision and reliability

Acknowledgements

We would like to thank the DLR for providing us with the high-resolution TanDEM-X DEM for our data processing (Proposal ID DEM_HYDR1727) and the ESA and Copernicus for making Sentinel-1 and Sentinel-2 data freely available to the public. We are especially grateful to the Deutsche Forschungsgemeinschaft (DFG) for funding our work as part of the Sino-German project Geo-ecosystems in transition on the Tibetan Plateau (TransTiP; GRK 2309/1). We thank our Chinese colleagues, especially at the NAMORS research station, who have worked tirelessly to support us before and during our field work.

References

Bateson, L., Cigna, F., Boon, D. & A. Sowter (2015): The application of the Intermittent SBAS (ISBAS) InSAR method to the South Wales Coalfield, UK. International Journal of Applied Earth Observation and Geoinformation, 34, 249-257, https://doi.org/10.1016/j.jag.2014.08.018.

Berardino, P., Fornaro, G., Lanari, R. & E. Sansosti (2002): A new algorithm for surface deformation monitoring based on small baseline differential SAR interferograms. IEEE Transactions on geoscience and remote sensing, 40(11), 2375-2383, https://doi.org/10.1109/TGRS.2002.803792.

Crosetto, M., Monserrat, O., Cuevas-González, M., Devanthéry, N. & B. Crippa (2016): Persistent scatterer interferometry: A review. ISPRS Journal of Photogrammetry and Remote Sensing, 115, 78-89, https://doi.org/10.1016/j.isprsjprs.2015.10.011.

Daanen, R. P., Grosse, G., Darrow, M. M., Hamilton, T. D. & B. M. Jones (2012): Rapid movement of frozen debris-lobes: implications for permafrost degradation and slope instability in the south-central Brooks Range, Alaska. Natural Hazards and Earth System Sciences, 12(5), 1521-1537, https://doi.org/10.5194/nhess-12-1521-2012.

Fialko, Y., Simons, M., & D. Agnew (2001): The complete (3-D) surface displacement field in the epicentral area of the 1999 Mw7. 1 Hector Mine earthquake, California, from space geodetic observations. Geophysical research letters, 28(16), 3063-3066, https://doi.org/10.1029/2001GL013174.

Haeberli, W., Noetzli, J., Arenson, L., Delaloye, R., Gärtner-Roer, I., Gruber, S., Isaksen, K., Kneisel, C., Krautblatter, M. & M. Phillips (2010): Mountain permafrost: development and challenges of a young research field. Journal of Glaciology, 56(200), 1043-1058, https://doi.org/10.3189/002214311796406121.

Hauck, C. & D. Von der Mühll (2003): Evaluation of geophysical techniques for application in mountain permafrost studies, Zeitschrift für Geomorphol. N.F., 132, 161–190.

Hock, R., G. Rasul, C. Adler, B. Cáceres, S. Gruber, Y. Hirabayashi, M. Jackson, A. Kääb, S. Kang, S. Kutuzov, A. Milner, U. Molau, S. Morin, B. Orlove, & H. Steltzer (2019): High Mountain Areas. In: IPCC Special Report on the Ocean and Cryosphere in a Changing Climate [H.-O. Pörtner, D.C. Roberts, V. Masson-Delmotte, P. Zhai, M. Tignor, E. Poloczanska, K. Mintenbeck, A. Alegría, M. Nicolai, A. Okem, J. Petzold, B. Rama & N.M. Weyer (eds.)].

Jarvis, A., Reuter, H. I., Nelson, A. and Guevara, E. (2008): Hole-filled SRTM for the globe Version 4, International Centre for Tropical Agriculture (CIAT), available from http://srtm.csi.cgiar.org.

Kneisel, C., Hauck, C., Fortier, R. & B. Moorman (2008): Advances in Geophysical Methods for Permafrost Investigations, , 178(March), 157–178, https://doi.org/10.1002/ppp.616.

Mewes, B., Hilbich, C., Delaloye, R. & C. Hauck (2017): Resolution capacity of geophysical monitoring regarding permafrost degradation induced by hydrological processes, Cryosphere, 11(6), 2957–2974, http://dx.doi.org/10.5194/tc-11-2957-2017, 2017.

Notti, D., Herrera, G., Bianchini, S., Meisina, C., García-Davalillo, J. C. & F. Zucca (2014): A methodology for improving landslide PSI data analysis. International Journal of Remote Sensing, 35(6), 2186-2214, https://doi.org/10.1080/01431161.2014.889864.

Reinosch, E., Buckel, J., Dong, J., Gerke, M., Baade, J., & B. Riedel (2019): InSAR time series analysis of seasonal surface displacement dynamics on the Tibetan Plateau, The Cryosphere Discuss., https://doi.org/10.5194/tc-2019-262, in review.

Yao, T., Liu, X., Wang, N. & Y. Shi (2000): Amplitude of climatic changes in Qinghai-Tibetan Plateau. Chinese Science Bulletin, 45(13), 1236-1243, https://doi.org/10.1007/BF02886087.

Von der Mühll, D., Hauck, C. & H. Gubler (2002): Mapping of mountain permafrost using geophysical methods, Prog. Phys. Geogr., 26(4), 643–660, https://doi.org/10.1191/0309133302pp356ra.

Wu, Q., Zhang, T. & Y. Liu (2010): Permafrost temperatures and thickness on the Qinghai-Tibet Plateau. Global and Planetary Change, 72(1-2), 32-38, https://doi.org/10.1016/j.gloplacha.2010.03.001.

Contact

Eike Reinosch
Markus Gerke
Björn Riedel

TU Braunschweig
Institut für Geodäsie und Photogrammetrie
Bienroder Weg 81
38106 Braunschweig

Johannes Buckel
Andreas Hördt

TU Braunschweig
Institut für Geophysik und extraterrestrische Physik
Mendelssohnstr. 3
38106 Braunschweig

Jussi Baade

Friedrich-Schiller-Universität Jena
Institut für Geographie
Löbdergraben 32
07743 Jena